

Electron spectrum of magnetic interface structures based on narrow-gap semiconductors

N. Malkova

Institute of Applied Physics, AS of Moldova, 2028 Kishinev, Moldova

I. Gómez and F. Domínguez-Adame

GISC, Departamento de Física de Materiales, Universidad Complutense, E-28040 Madrid, Spain

(Received 1 August 2000; published 2 January 2001)

In this work we deal with magnetic junction structures in which a homogeneous narrow-gap semiconductor is subjected to an inhomogeneous magnetic field. The aim of the paper is to elucidate magnetic field effects on the electron energy spectrum of narrow-gap semiconductors in inhomogeneous magnetic fields. The two-band Dirac model is used as a model Hamiltonian. Spectra and wave functions for the magnetic junction are obtained. Wave functions for the lowest quasi Landau levels are strongly localized near the interface plane showing the characteristic properties of snake orbits. The spin properties of the quasi Landau levels are studied.

DOI: 10.1103/PhysRevB.63.035317

PACS number(s): 73.20.-r, 73.21.-b, 75.70.Cn

I. INTRODUCTION

Recent experimental techniques have opened up the way to experiments in inhomogeneous magnetic fields with periods in the nanometer region.¹ This kind of field has been realized with the fabrication of magnetic dots, patterning of ferromagnetic materials, and deposition of superconducting materials on conventional heterostructures. Increased interest in studying a two-dimensional electron gas (2DEG) subjected to inhomogeneous magnetic fields is mainly caused by the special tunneling and kinetic properties of magnetic structures. In contrast with tunneling through electric barriers, the tunneling probability of the magnetic structures depends not only on the electron momentum perpendicular to the tunneling barrier but also on its momentum parallel to the barrier. This renders the tunneling an inherently two-dimensional process where magnetic barriers possess wave-vector filtering properties.² Related to this subject is the effect of a local magnetic field on the tunneling current through a thick potential barrier considered in Ref. 3. A magnetic field strictly localized within a potential barrier was shown to lead to resonances centered within the barrier. A number of papers have considered quantum transport of a 2DEG in a weak magnetic field modulation. Magnetoresistance commensurability oscillations (so-called Weiss oscillations) in these systems were first theoretically predicted⁴ and then observed in experimental studies of 2DEG's in periodically modulated magnetic fields.¹ The reason for the oscillations is the commensurability between the classical cyclotron diameter and the period of the modulation.⁵ It is worth noting, as well, the observation of the very large, low-field magnetoresistance of a 2DEG subjected to a periodic magnetic field that alternates in sign.⁶

Moreover, the interest in electron properties of the 2DEG in alternating magnetic fields is motivated by the relevance of the problem to the composite-fermion description of a half-filled Landau level as a classical analog of the fractional quantum Hall effect.^{7,8} As a matter of fact, for a density modulated 2DEG, which is supposed to be in the fractional quantum Hall regime,^{9,10} the problem reduces to the ballistic motion of composite fermions moving in a periodic magnetic

field. A quasiclassical treatment of the problem results in considering states that are referred to as snake states due to the characteristic shape of the classical analog trajectories. Müller¹¹ seems to have been the first to give a quantum-mechanical treatment for the snake states in a constant-gradient field. In the presence of a uniform magnetic field, electrons of an infinitely large 2DEG are well known to be localized on cyclotron orbits.¹² Conduction is zero in the absence of scattering and sample boundaries. A spatially nonuniform magnetic field can result in extended (snake) states. Snake orbits in semiconductor devices have been considered in detail theoretically in a recent work.¹³ Experimental proof of the existence of snake states propagating along lines of zero magnetic field has been obtained from electron transport perpendicular to the interface in Refs. 1 and 6.

In their very nature the unusual tunneling and kinetic properties of the magnetic structures result from the rearrangement of the band spectrum under inhomogeneous magnetic fields. To our knowledge, theoretical works relevant to the electron transport problem of magnetic structures have treated a single-band model to describe the energy spectrum, any spin properties of the band structure being neglected. As a matter of fact this approximation is valid for semiconductors like GaAs because in this case for the magnetic fields between 0.1 and 1 T used in experiments the forbidden gap is larger than the cyclotron energy. But the situation will change for the narrow-gap semiconductors of type III-V, IV-VI, and II-VI. For example, for InSb the cyclotron energy will already be larger than the value of the gap at $B \sim 1$ T. Two-band effects are even more evident for the IV-VI and II-VI narrow-gap semiconductors or their solid solutions in which a gapless state can be reached. Obviously, if a magnetic field is applied to the system of a narrow-gap semiconductor, the single-band model can lead to an inadequate description of transport effects.

In this work we are concerned with magnetic structures in which a homogeneous narrow-gap semiconductor is subjected to an inhomogeneous magnetic field. Our aim is to provide a clear picture of alternating magnetic field effects on the electron energy spectrum of narrow-gap semiconductors. For the magnetic structures considered, the magnetic

field is taken to be directed along the z axis, being homogeneous along the y axis and varying along the x axis. As a first step in studying the inhomogeneous magnetic field, we do not take into account a realistic profile of the changing of the magnetic field and consider the simplest situation of a step-like interface. The reason for this approximation is the following. As shown,² by the proper choice of the experimental parameters it is possible to realize such a sharp magnetic interface that its width is less than the characteristic magnetic length l_H (which for values of the magnetic field up to 10 T cannot be less than 10 nm).

Two different magnetic junction structures are considered. The first one is a so-called inverted magnetic junction where $B_+B_- < 0$ [$B_\pm \equiv B_z(x = \pm\infty)$]. The second structure is a normal magnetic junction where $B_-B_+ > 0$.

This paper is organized as follows. In Sec. II we describe our theoretical model. The band spectrum and wave functions for the inverted and normal magnetic junctions are obtained. In Sec. III spin properties of the electron states are studied. Section IV concludes the paper with a brief summary of the main results.

II. TWO-BAND MODEL

The simplest theoretical approach for the narrow-gap semiconductors is known to be a two-band model,¹⁴ which in the first approximation of the $\mathbf{k} \cdot \mathbf{p}$ perturbation theory reduces to the following Dirac Hamiltonian:

$$\mathcal{H}_0 = \begin{pmatrix} \Delta + V & -i\hbar v \boldsymbol{\sigma} \cdot \mathbf{k} \\ i\hbar v \boldsymbol{\sigma} \cdot \mathbf{k} & -\Delta + V \end{pmatrix}. \quad (1)$$

Here Δ is determined as the half band gap, $\Delta = E_g/2$; V is the so-called work function, describing the shift of the gap middles; \mathbf{k} is the momentum operator, $\mathbf{k} = -i\nabla$; v is the interband matrix element of the velocity operator; $\boldsymbol{\sigma} = (\sigma_x, \sigma_y, \sigma_z)$ is the vector whose components are the Pauli matrices. In the simplest form this two-band Dirac Hamiltonian defines two nearby conduction and valence bands as two Kramers conjugate states. Therefore, the Hamiltonian (1) takes into account spin properties of the wave functions, called eigenspinors in this case.

In this work we neglect the Zeeman term in the Hamiltonian in the presence of a magnetic field. Thus, a static magnetic field is incorporated in \mathcal{H}_0 just by the standard substitution

$$\mathbf{k} \rightarrow \mathbf{k} + \frac{e}{\hbar c} \mathbf{A}(\mathbf{r}). \quad (2)$$

For the magnetic field $\mathbf{B} = (0, 0, B_z)$ the electromagnetic vector potential \mathbf{A} is chosen in the Landau gauge as $\mathbf{A}(\mathbf{r}) = (0, xB_z, 0)$. Following the results of Ref. 15 we write the four bulk eigenfunctions for Eq. (1) in the form

$$\Psi^\pm(\mathbf{r}) = e^{i(k_y y + \chi_\xi \xi)} \begin{pmatrix} c_1 D_{p-1}(\pm \xi) \mathbf{u} + c_2 D_p(\pm \xi) \mathbf{v} \\ c_3 D_{p-1}(\pm \xi) \mathbf{u} + c_4 D_p(\pm \xi) \mathbf{v} \end{pmatrix}, \quad (3)$$

where the columns vectors \mathbf{u} and \mathbf{v} are defined by

$$\mathbf{u} = \frac{1}{2} \begin{pmatrix} 1 + \varphi \\ 1 - \varphi \end{pmatrix}, \quad \mathbf{v} = \frac{1}{2} \begin{pmatrix} 1 - \varphi \\ 1 + \varphi \end{pmatrix}. \quad (4)$$

Here a new dimensionless variable is introduced by $\xi = \sqrt{2}(x_0 + x)/l_H$, $x_0 = \varphi k_y l_H^2$ is the center of the Landau orbits, $\varphi = \text{sgn}(B_z) = \pm 1$ is the orientation of the magnetic field ($\varphi = 1$ corresponds to a field pointing along the positive z axis), $l_H = \sqrt{\hbar c/e|B_z|}$ is the magnetic length, and $\chi_\xi = l_H k_z$ and $\xi = z/l_H$ are the dimensionless z momentum and coordinate. The functions $D_p(\pm \xi)$ are the parabolic cylinder functions. They constitute two independent, nonorthogonal solutions of the harmonic-oscillator equation

$$\left(-\frac{d^2}{d\xi^2} + \frac{\xi^2}{4} \right) D_p(\xi) = \left(p + \frac{1}{2} \right) D_p(\xi), \quad (5)$$

and the corresponding bulk dispersion relation is

$$\chi_\xi^2 + 2p = \left[\frac{l_H}{\hbar v} \right]^2 [(E - V)^2 - \Delta^2], \quad (6)$$

where p is determined from the boundary conditions.

The spinor coefficients in Eq. (3) are given by

$$\begin{bmatrix} c_1 \\ c_2 \\ c_3 \\ c_4 \end{bmatrix} = \begin{bmatrix} \begin{bmatrix} 1 \\ \pm \frac{1}{\sqrt{p}} \end{bmatrix} \\ \frac{i\hbar v}{E - V + \Delta} (\mathbf{k}_p^\pm \cdot \boldsymbol{\sigma}) \begin{bmatrix} 1 \\ \pm \frac{1}{\sqrt{p}} \end{bmatrix} \end{bmatrix}, \quad (7)$$

where $\mathbf{k}_p^\pm = (1/l_H)(\pm i(1-p)/\sqrt{2}, \pm(1+p)/\sqrt{2}, \chi_\xi)$.

Starting from the Schrödinger equation determined by the Hamiltonian (1) with the replacement (2), we look for a solution as a linear combination of eigenfunctions (3). For a steplike magnetic interface with a sharp change of the magnetic field at $x=0$, boundary conditions need to be applied to the eigenvalue problem. Assuming the wave function to be continuous at the interface and integrating the Schrödinger equation across the interface boundary, we obtain the boundary conditions reduced just to the demand for wave function continuity. Moreover, we should take into account that the two solutions $D_p(\pm \xi)$ present different asymptotic behaviors at $\xi(x) \rightarrow \pm\infty$. Since the solution must decay far away from the interface the wave function is allowed to include only Ψ^+ functions for $x > 0$. Meanwhile, only Ψ^- functions are allowed for $x < 0$.

A. Inverted magnetic junction

For the inverted magnetic junction $B_+ = -B_- = B$, the dispersion relation reads

$$D_p^2(\xi_0) - p D_{p-1}^2(\xi_0) = 0, \quad (8)$$

where $\xi_0 = \sqrt{2}k_y l_H$ is the dimensionless x coordinate of the Landau orbit center. This equation defines for every energy

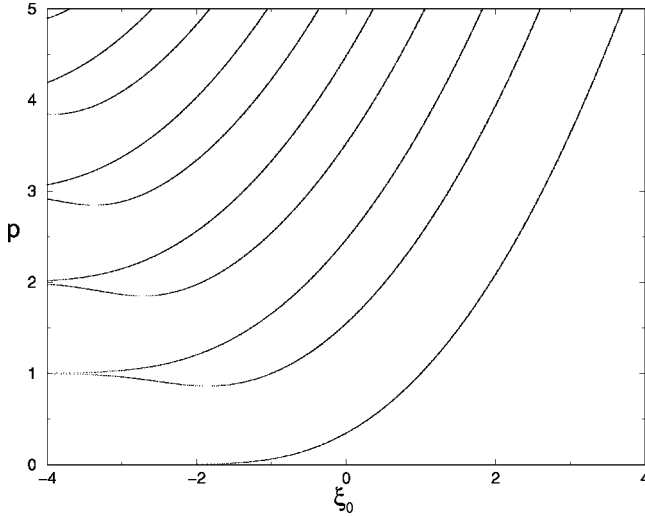


FIG. 1. Energy spectrum of the symmetrical inverted magnetic junction.

the allowed values of the momentum k_y related to the location of the Landau orbit centers.

The numerical solution of this dispersion relation is shown in Fig. 1 where the allowed values of p are shown as a function of ξ_0 . Taking into account the dependence of E on p [Eq. (6)] we can consider this figure as a band spectrum. The case of a quasiclassical magnetic field when $\varepsilon_F = 4\hbar\omega_H$ (ε_F is the Fermi energy, ω_H is the cyclotron frequency) is studied. The following parameters have been used: $\varepsilon_F = \Delta = 0.1$ eV. In the case of the 2DEG (that is, $\chi_\zeta = 0$), Eq. (6) implies that $(E - V)/\Delta = \sqrt{p+1}$.

We note that the energy spectrum of the inverted magnetic junction consists of successive bands that are the remnants of the Landau levels showing a time-reversal asymmetry.¹¹ The energy spectrum shown in Fig. 1 has a direct analogy with the single-band model¹³ and can be interpreted in the same way. For the 2DEG under a step magnetic field the single-band problem is reduced to solving the one-dimensional Schrödinger equation

$$\left[\frac{1}{2m} \frac{d^2}{dx^2} - V_{k_y}(x) + E \right] \psi(x) = 0$$

with the effective potential

$$V_{k_y}(x) = \left\{ k_y - x \left[1 - \left(1 - \frac{B_+}{B_-} \right) \theta(x) \right] \right\}^2,$$

which depends on k_y . We analyze the energy spectrum of the inverted magnetic junction (see Fig. 1) in terms of the effective potential V_{k_y} . For $k_y \ll 0$ the potential has the form of two decoupled parabolic wells. Thus, we obtain the Landau states $(n+1/2)\hbar\omega_H$ as a solution; they are twofold degenerate because of the identity of the states in both parabolic wells. These states have zero velocity $v_y = (1/\hbar)(\partial E_{n,k_y}/\partial k_y)$ along the y axis.

With increasing k_y the parabolic wells become coupled. As a result the wave function becomes localized near the

interface. These states are characterized by nonzero velocity v_y and have snake orbits going back and forth around the interface through the B_+ and B_- regions. The velocity v_y of these states increases with k_y .

As was noted in this consideration the Zeeman term is neglected. Each quasi Landau level is doubly degenerate and described by two wave functions. The squared modulus of one of the normalized wave functions on each side of the interface reads

$$|\Psi^\pm|^2 = \frac{1}{\sqrt{2}l_H I} \left\{ 1/p D_p^2(\pm\xi) + D_{p-1}^2(\pm\xi) \mp \frac{\Delta}{E-V} [D_{p-1}^2(\pm\xi) - 1/p D_p^2(\pm\xi)] \right\}. \quad (9)$$

Here $\Psi^+ = \Psi(x > 0)$, $\Psi^- = \Psi(x < 0)$, $\pm\xi = (\sqrt{2}/l_H)(x_0 \pm x)$, and

$$I = \int_{\xi_0}^{\infty} \left[D_{p-1}^2(y) + \frac{1}{p} D_p^2(y) \right] dy.$$

The analytical expression for the probability density function of the spin conjugate state $\tilde{\Psi}$ is written in the same form with a sign change in the second term in Eq. (9).

The probability density functions for the four lowest quasi Landau levels at $\xi_0 = -2, 0, 2$ are shown in Fig. 2. Here the probability density functions for the different levels are shifted upward with respect to each other and ordered by their corresponding energy. It can be seen that the value of ξ_0 determines not only the location of the cyclotron orbit centers but also the extension of the quasi Landau states, namely, the larger the value of ξ_0 the more the wave function becomes localized. This fact is well understood from the analysis of the profile of the effective potential. As follows from Fig. 2(a), at $\xi_0 = -2$ when the electrons experience the double-well effective potential, the wave function for the excited states is not symmetrical, but at $\xi_0 = 0$ [Fig. 2(b)] and $\xi_0 = 2$ [Fig. 2(c)] the electrons experience a symmetrical coupled effective potential; as a result their wave function becomes symmetrical.

B. Normal magnetic junction

For the normal magnetic junction the magnetic field just changes its absolute value at the interface boundary. The solution of the boundary value problem leads to the following dispersion relation:

$$l_H^- D_{q-1}(-\xi_0^-) D_p(\xi_0^+) + l_H^+ D_q(-\xi_0^-) D_{p-1}(\xi_0^+) = 0. \quad (10)$$

Here l_H^+ and l_H^- are the values of the magnetic length for $x > 0$ and $x < 0$, respectively, $\sqrt{q/p} = l_H^+/l_H^-$, and $\xi_0^\pm = \sqrt{2}k_y l_H^\pm$ are again the dimensionless x coordinates of the Landau orbit centers on different sides of the interface boundary.

The numerical solution of Eq. (10) is presented in Fig. 3. The calculations were performed for two different values of the parameter $\beta = l_H^+/l_H^-$, namely, $\beta = 0.5$ in Fig. 3(a) and

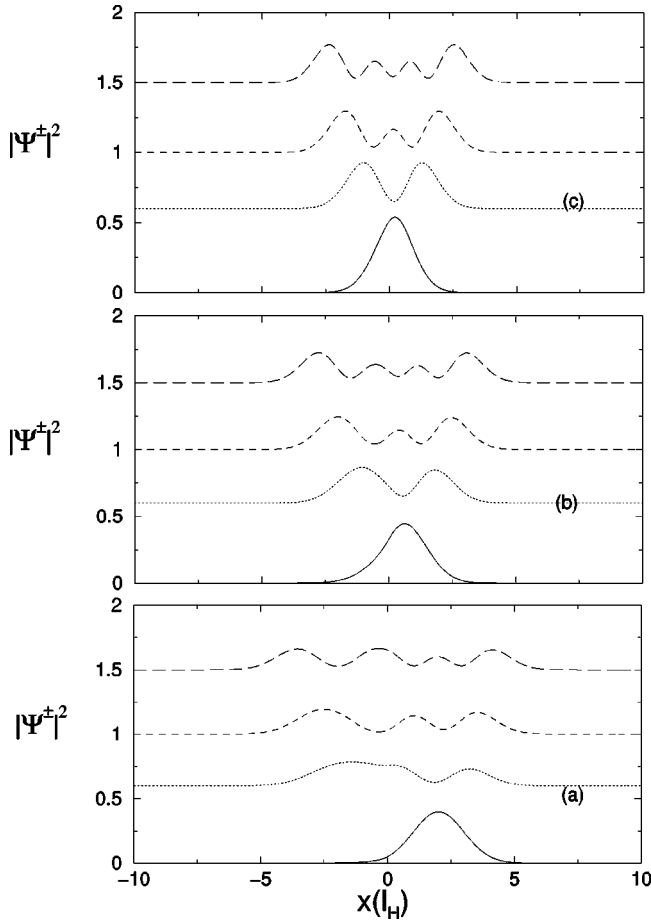


FIG. 2. Wave functions of the symmetrical inverted magnetic junction for the lowest quasi Landau levels at the points (a) $\xi_0 = -2$, (b) 0, and (c) 2.

$\beta=0.9$ in Fig. 3(b). The energy spectrum now is qualitatively different from the previous case. First, we note that the k_y states are no longer degenerate at $k_y \leq 0$ (but they are still doubly spin degenerate). Second, for $k_y \geq 0$ the energy levels approach the Landau levels for states in a uniform magnetic field B_+ . Third, the electron velocity along the y direction

(the slope of the dispersion curves) depends on the value of β . The larger β , the smaller is the electron velocity. At $\beta \rightarrow 1$ the electron velocity vanishes and consequently snake states disappear.

We can analyze this spectrum as coming from the effective potential again. The velocity of the snake orbits is strongly reduced now, and it is going to zero at $k_y \geq 0$ and $k_y \leq 0$ for all quasi Landau levels. The probability density functions for the lowest quasi Landau levels for $\beta=0.5$ are shown in Fig. 4 at $\xi_0=2$ and $\xi_0=0$. We can see an expected result: in both cases the electrons are in snake states localized near the interface boundary, being more localized at $\xi_0=0$ than at $\xi_0=2$.

III. SPIN

From this two-band model, in which the spin properties of the wave functions are directly characterized by the eigenstates, we can find the average value of the spin vector

$$\langle \mathbf{S}(x) \rangle = \langle \Psi | \hat{\Sigma} | \Psi \rangle, \quad (11)$$

where $\hat{\Sigma}$ is the spin operator. After simple calculations we obtain that the three components of the average spin vector for each value of k_y do not vanish, even in the case of a symmetrical inverted magnetic junction. Of course, the direction of these vectors for each of the two spin-conjugate states is opposite to each other. For the 2DEG (that is, $\chi_\zeta = 0$) in the case of the inverted magnetic junction, we obtain

$$\langle \mathbf{S}(x) \rangle = (0, 0, S_z(\xi)),$$

where

$$S_z^\pm(\xi) = \frac{1}{\sqrt{2}l_H I} \left\{ \mp \frac{1}{p} D_p^2(\pm \xi) - D_{p-1}^2(\pm \xi) - \frac{\Delta}{E-V} [D_{p-1}^2(\pm \xi) + 1/p D_p^2(\pm \xi)] \right\}.$$

After integrating along x we have

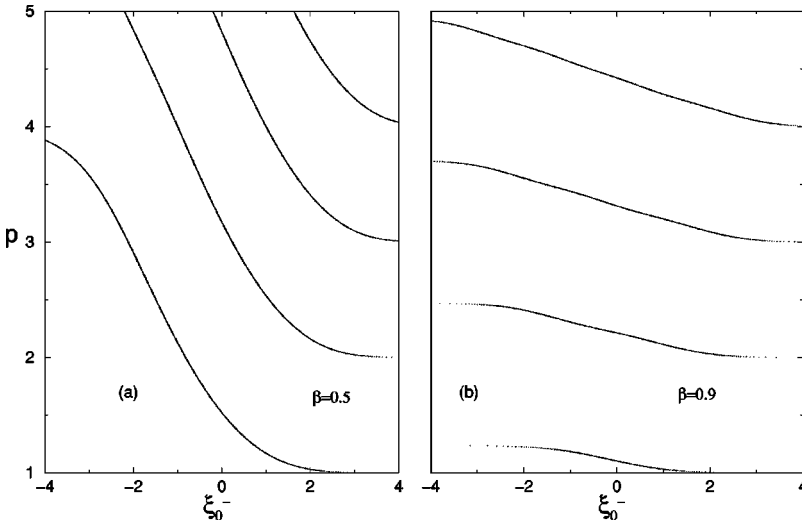


FIG. 3. Energy spectrum of the normal magnetic junction for (a) $\beta=0.5$ and (b) 0.9.

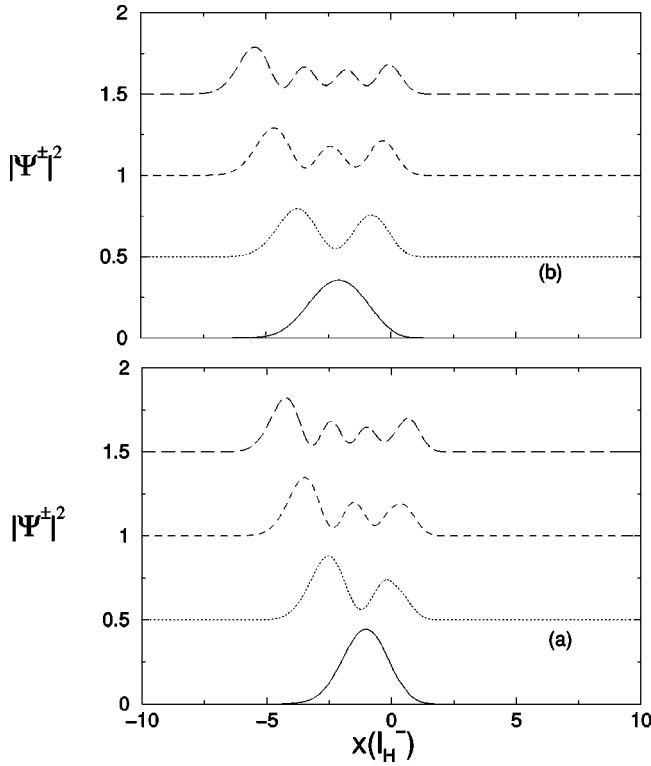


FIG. 4. Wave function of the normal magnetic junction for $\beta = 0.5$ at the points (a) $\xi_0 = 0$ and (b) $\xi_0 = 2$.

$$\langle S_z \rangle = -\frac{\Delta}{E - V}. \quad (12)$$

It follows that, despite the fact that in the symmetrical inverted magnetic junction the number of electrons with spin up and down should be the same, the spin of each of the spin-conjugate states happens to be a nonzero vector. Moreover, the absolute value of this vector changes for different values of ξ_0 . The spin value as a function of x for the inverted magnetic junction at $\xi_0 = 0$ and at $\xi_0 = 2$ is shown in Fig. 5. As follows from this figure the spin of the snake states (which are the states at $\xi_0 = 0$ and $\xi_0 = 2$) is a function localized near the magnetic interface boundary. Obviously, the other spin-conjugate state $\tilde{\Psi}$ has the opposite spin direction, resulting in a zero value of the spin sum. Figure 6 shows the average along the x direction of the spin as a function of ξ_0 for the two spin-conjugate states $\langle \tilde{S}_z \rangle = \Delta / (E - V)$ corresponding to the first quasi Landau level. We note that the average spin of the delocalized states ($k_y \ll 0$) tends to ± 1 for the two degenerate states and it decreases slowly up to $\sim \pm 0$ for the snake states ($k_y \gg 0$). When the Zeeman term is included the spin degeneracy will be removed. As a result, each of the quasi Landau levels of the magnetic junction will be characterized by a nonzero value of the average spin, which will be localized near the interface boundary for the snake states.

IV. SUMMARY

The electron energy spectrum of magnetic junctions based on narrow-gap semiconductors has been studied in some de-

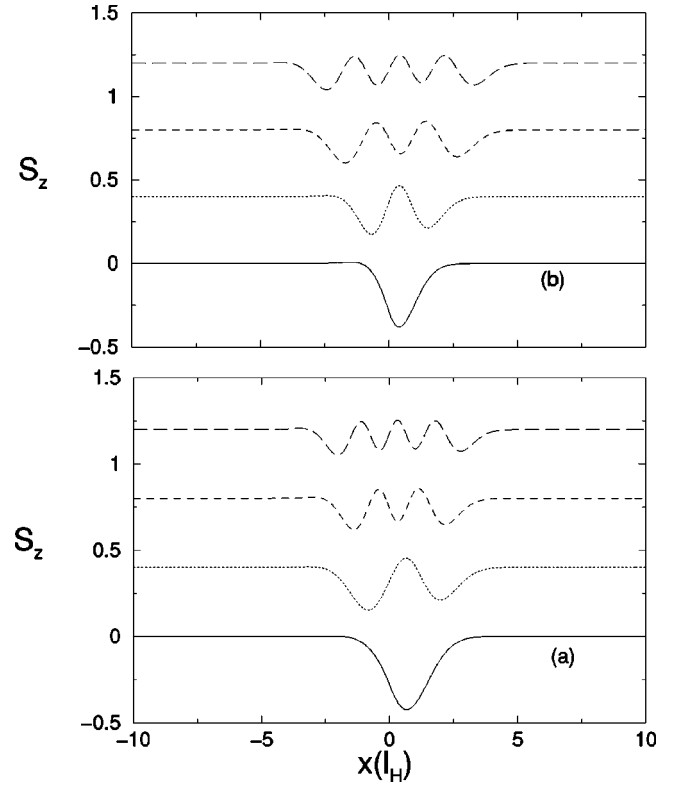


FIG. 5. Average spin of the inverted magnetic junction as a function of x at the points (a) $\xi_0 = 0$ and (b) 2.

tail. A two-band Dirac Hamiltonian has been used as a model. For a homogeneous magnetic field, the degenerate Landau levels have been shown to be transformed into bands of finite width in the case of a steplike magnetic field. The dispersion of these quasi Landau bands reveals time-reversal asymmetry.

In the symmetrical inverted magnetic junction the electron states at $k_y > 0$ travel freely along the interface resulting in an increase of the conductivity in the direction of the interface. In the case of the normal magnetic junction the

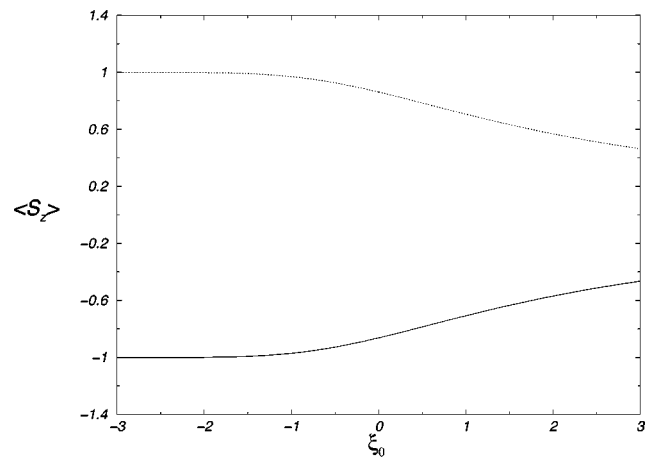


FIG. 6. Spin averaged along x direction of the inverted magnetic junction as a function of ξ_0 for the Ψ (solid line) and $\tilde{\Psi}$ (dashed line) spin degenerate states.

electron velocity along the junction depends on l_H^+/l_H^- going to zero as $k_y \rightarrow \pm\infty$.

The average spin of the quasi Landau levels of the magnetic junctions is a nonzero vector, being a function localized near the interface boundary for the snake states. In this way snake states can be considered as a quasi-one-dimensional spin system. When the Zeeman term was included, we were unable to find an analytical solution in the common case, but a calculation can be quite easily performed for the 2DEG ($\chi_\zeta=0$). It is obvious that the twofold degenerate levels split by the energy $\sim \hbar \omega_H$, removing their degeneracy. The spectrum will consist of a set of successive levels with opposite spin directions. As a result, given the energy ε_F , the snake states localized near the interface boundary will follow one after another, alternating the spin direction. We suppose that

in this way spin-dependent transport can be observed. But this effect demands a thorough study, which will be the subject of our next publication.

We conclude that the band spectrum of the magnetic junction based on a narrow-gap semiconductor, which was obtained in the framework of the two-band model, can be clearly interpreted from the shape of the effective potential. The energy spectrum and wave functions do not change dramatically in comparison with the single-band model. This provides the proof of the close connection between these models and makes us confident that the spin properties of magnetic interface structures that follow directly from the two-band model will find theoretical and experimental evidence in resonance splitting, magnetoresistance oscillation peaks, and tunneling transmission coefficients.

¹P.D. Ye, D. Weiss, R.R. Gerhardt, M. Seeger, K. von Klitzing, K. Eberl, and H. Nickel, Phys. Rev. Lett. **74**, 3013 (1995).

²A. Matulis, F.M. Peeters, and P. Vasilopoulos, Phys. Rev. Lett. **72**, 1518 (1992).

³V.M. Ramaglia, A. Tiaglicozzo, F. Ventriglia, and G.P. Zucchelli, Phys. Rev. B **43**, 2201 (1991).

⁴F.M. Peeters and P. Vasilopoulos, Phys. Rev. B **47**, 1466 (1993).

⁵C.W.J. Beenakker, Phys. Rev. Lett. **62**, 2020 (1989).

⁶A. Nogaret, S. Carlton, B.L. Gallagher, P.C. Main, M. Henini, R. Wirtz, R. Newbury, M.A. Howson, and S.P. Beaumont, Phys. Rev. B **55**, R16 037 (1997).

⁷I.S. Ibrahim and F.M. Peeters, Phys. Rev. B **52**, 17 321 (1995).

⁸F. Evers, A.D. Mirlin, D.G. Polyakov, and P. Wolfle, Phys. Rev. B **60**, 8951 (1999).

⁹D.B. Chklovskii and P.A. Lee, Phys. Rev. B **48**, 18 060 (1993).

¹⁰D.B. Chklovskii, Phys. Rev. B **51**, 9895 (1995).

¹¹J.E. Müller, Phys. Rev. Lett. **68**, 385 (1992).

¹²S. Datta, *Electron Transport in Mesoscopic Systems* (Cambridge University Press, Cambridge, 1995).

¹³F.M. Peeters, J. Reijniers, S.M. Badalian, and P. Vasilopoulos, Microelectron. Eng. **47**, 405 (1999).

¹⁴D. Agassi and V. Korenman, Phys. Rev. B **37**, 10 095 (1988).

¹⁵D. Agassi, Phys. Rev. B **49**, 10 393 (1994).